Biomaterials 33 (2012) 1363–1375

Contents lists available at SciVerse ScienceDirect

Biomaterials

journal homepage: www.elsevier.com/locate/biomaterials

The role of microstructured and interconnected pore channels in a collagen-based nerve guide on axonal regeneration in peripheral nerves

Ahmet Bozkurt [a,*,1], Franz Lassner [a,1], Dan O'Dey [a], Ronald Deumens [b,c], Arne Böcker [a], Tilman Schwendt [d], Christoph Janzen [e], Christoph V. Suschek [a], Rene Tolba [f], Eiji Kobayashi [g], Bernd Sellhaus [b], S. Tholl [h], Lizette Eummelen [h], Frank Schügner [h], Leon Olde Damink [h], Joachim Weis [b], Gary A. Brook [b], Norbert Pallua [a]

[a] Department of Plastic Surgery, Reconstructive and Hand Surgery, Burn Center, Medical Faculty, RWTH Aachen University, Pauwelsstrasse 30, 52074 Aachen, Germany
[b] Institute for Neuropathology, University Hospital, Medical Faculty, RWTH Aachen University, Aachen, Germany
[c] Department of Anesthesiology, Maastricht University Medical Center, Maastricht, The Netherlands
[d] Fraunhofer Institute for Laser Technology, Aachen University of Technology, Aachen, Germany
[e] Chair of Laser Technology, Aachen University of Technology, Aachen, Germany
[f] Institute for Laboratory Animal Research, Medical Faculty, RWTH Aachen University, Aachen, Germany
[g] Center for Development of Advanced Medical Technology, Jichi Medical University, Tochigi, Japan
[h] Matricel GmbH, Herzogenrath, Germany

ARTICLE INFO

Article history:
Received 19 October 2011
Accepted 24 October 2011
Available online 13 November 2011

Keywords:
Nerve regeneration
Schwann cells
Scaffold
Neurotmesis
Sciatic nerve
Bands of Büngner

ABSTRACT

The use of bioengineered nerve guides as alternatives for autologous nerve transplantation (ANT) is a promising strategy for the repair of peripheral nerve defects. In the present investigation, we present a collagen-based micro-structured nerve guide (Perimaix) for the repair of 2 cm rat sciatic nerve defects. Perimaix is an open-porous biodegradable nerve guide containing continuous, longitudinally orientated channels for orientated nerve growth. The effects of these nerve guides on axon regeneration by six weeks after implantation have been compared with those of ANT. Investigation of the regenerated sciatic nerve indicated that Perimaix strongly supported directed axon regeneration. When seeded with cultivated rat Schwann cells (SC), the Perimaix nerve guide was found to be almost as supportive of axon regeneration as ANT. The use of SC from transgenic green-fluorescent-protein (GFP) rats allowed us to detect the viability of donor SC at 1 week and 6 weeks after transplantation. The GFP-positive SC were aligned in a columnar fashion within the longitudinally orientated micro-channels. This cellular arrangement was not only observed prior to implantation, but also at one week and 6 weeks after implantation. It may be concluded that Perimaix nerve guides hold great promise for the repair of peripheral nerve defects.

1. Introduction

The peripheral nervous system has an intrinsic ability to regenerate following injury. When the continuity of the endoneurium is maintained, regenerating axons are guided from the proximal to the distal nerve stump through preserved connective tissue elements. Schwann cell (SC) proliferation within the endoneurial tubes of the distal nerve generates the Bands of Büngner [1]. These aligned Schwann cell tubes guide the regenerating axons to their appropriate distal target organs and support functional recovery [2]. However, when peripheral nerve injury (PNI) leads to a gap, including discontinuity of the perineurium and epineurium, nerve regeneration is severely hampered. Only few, if any, axons reach the distal nerve stump. In such cases, surgical intervention is required to promote axon regeneration.

Direct nerve suture repair (nerve coaptation) is the preferred clinical treatment for short nerve defects. However, in the case of large nerve defects (where tensionless nerve repair is not possible) the interposition of a bridge between the proximal and distal nerve stumps is required. An autologous donor nerve, usually a sensory nerve (e.g. sural nerve [3]), is chosen to bridge such gaps. Despite its gold standard status, autologous nerve transplantation (ANT) is not

* Corresponding author. Tel.: +49 241 800; fax: +49 241 82448.
E-mail addresses: abozkurt@ukaachen.de, abozkurt77@gmx.de (A. Bozkurt).
[1] First authors.

0142-9612/$ – see front matter © 2011 Elsevier Ltd. All rights reserved.
doi:10.1016/j.biomaterials.2011.10.069

ideal for a number of reasons, including specific- (e.g. loss of sensory function) and general- (wound infection, haematoma, scarring, wound pain etc.) co-morbidities at the donor site. Furthermore, the availability of donor nerves is limited and unwanted complications may develop, including neuropathic pain [4]. Interestingly, only 40–50% of patients regain useful function when treated with autologous nerves [5]. Therefore, a wide range of materials, both biological and synthetic, have been investigated as alternatives to ANT in the repair of peripheral nerve defects [3].

The therapeutic effect of a bridging material in the repair of PNI can be influenced by its ability to physically and biochemically mimic aspects of the lost peripheral nerve. Such considerations have led to a tissue repair concept containing at least two essential components, as summarized by Lundborg [6]. Firstly, nerve guides should ideally contain an orientated matrix or scaffold. This can act as replacement for the endoneurial tubes, providing guidance and mechanical support for directed SC migration and axonal growth. Secondly, nerve guides should contain growth factors. These can either be produced by cells (e.g. by cultured- or migrating, endogenous SC) or be incorporated into the matrix for stimulation of effective and orientated axonal growth.

Although a large number of investigations have used hollow conduits as bridging devices, a growing body of interest has emerged in the development of micro- or nanostructured scaffolds [7]. A similar principle has also been devised for the repair of traumatically injured central nervous system. For example, a multi-component polymer scaffold seeded with neural stem cells has been designed to assist in the repair of traumatically injured spinal cord [8]. We have recently described the *in vitro* characteristics of a collagen-based micro-structured scaffold (Perimaix) containing continuous, longitudinally orientated and interconnected pores [9]. The structure of the scaffold has been designed to resemble the geometric dimensions of a peripheral nerve and 3D tissue culture experiments revealed it to be an excellent substrate for orientated axon outgrowth [10,11]. In earlier studies, two forms of the scaffold (termed Perimaix-17% and Perimaix-33%), differing in physical and molecular properties, were seeded with highly enriched populations of SC. The SC survived and formed aligned columns which followed the longitudinal orientation of the scaffold's internal microstructure, resembling Bands of Büngner. In the present investigation, the properties of Perimaix-17% (PM-17) and Perimaix-33% (PM-33) have been assessed in an *in-vivo* model of PNI. The model uses the epineurium of the lesioned rat sciatic nerve to secure and maintain the position of the implanted scaffold for the duration of the experiment. The hypothesis tested was that Perimaix nerve guides could promote directed axonal growth across 2 cm long nerve defects.

2. Materials and methods

All experiments were conducted in accordance with national- and EU regulations regarding animal care. Experimental animals were housed in a temperature- and humidity-controlled environment with a cycle of 12 h (h) light and 12 h darkness, and allowed free access to food and water. Every attempt was made to minimize the number of animals used, as well as any pain and discomfort that they may feel. Female inbred Lewis rats (12 weeks old, Charles River, Germany) and female transgenic rats (Lewis rat background) expressing green fluorescent protein (GFP) were used in the study. The transgenic GFP rats were provided by Prof. E. Kobayashi, (Jichi Medical University, Japan) and the husbandry and genotyping were performed by Prof. R. Tolba (Institute for Laboratory Animal Science, RWTH Aachen University). GFP transgenic rats were used at the age of 10–12 weeks for obtaining GFP-expressing Schwann cells (GFP/SC) [12].

2.1. Isolation of Schwann cells

SC were isolated and expanded *in vitro* as described earlier [13]. Briefly, both sciatic nerves were removed from terminally anaesthetized rats. The nerves were chopped into small pieces (1–2 mm) and were placed in Petri dishes in standard medium consisting of Dulbecco's modified essential medium (DMEM; Invitrogen™, Karlsruhe, Germany) supplemented with 10% foetal calf serum (FCS; PAA™, Pasching, Austria) and 1% Penicillin/Streptomycin (10.000 U/mL of penicillin, 10 mg/mL Streptomycin; PAA™, Pasching, Austria). After 7 days of incubation at 37 °C, the sciatic nerve fragments were enzymatically digested by incubation in collagenase followed by trypsin-EDTA (0.25%). Dissociated cells were plated onto poly-L-lysine/laminin-coated culture flasks (pll/lam; both Sigma–Aldrich™, Munich, Germany) and maintained in growth medium (DMEM containing 10% FCS, 40 μg/ml transferrin, 41.69 μg/ml μg bFGF, 41.698 μg/ml heregulin, 472.5 ng/mlforskolin, 10 μg/ml insulin 0.1% gentamicin, 1% glutamax).

2.2. Purification of SC

To obtain highly enriched SC, cell purification was performed using the Magnetic Assisted Cell Sorting (MACS®) system (Miltenyi Biotec, Bergisch Gladbach, Germany). Flasks with unpurified cells (i.e. SC and fibroblasts) were washed with phosphate buffered saline (PBS) and incubated with trypsin (0.05%) for 5 min. The cells were collected in growth medium, centrifuged at 300×*g* for 5 min at 4 °C, and washed with PBS supplemented with 2 mM EDTA (PE). For SC selection, the cell suspension was incubated with 2 μL of undiluted polyclonal rabbit anti-mouse low affinity nerve growth factor-receptor antibody (p75/LNGFr Chemicon International Ltd, Hampshire, United Kingdom) in PE containing 0.5% BSA (PEB) for 10 min at 7 °C. At the end of the incubation period, the cells were centrifuged, washed and incubated with 20 μL microbead-linked rat anti-mouse IgG1 (diluted 1:500; Miltenyi Biotec, Bergisch Gladbach, Germany) in 80 μL PEB for 15 min at 7 °C. After two rinsing steps with PE, an MS-column (Miltenyi Biotec, Bergisch Gladbach, Germany) was placed in the MiniMACS® magnet (Miltenyi Biotec, Bergisch Gladbach, Germany) and flushed with PEB. A maximum of 10^7 cells were resuspended in 500 μL PEB and applied to the MS column followed by 3 rinses with 500 μL PEB to wash out unbound cells (i.e. p75/LNGFr-negative cells, mainly fibroblasts). After removal from the magnet, the column was flushed with 1 mL PE, which allowed the collection of the p75/LNGFr-positive, Schwann cell fraction. The high purity (>95%) of the p75/LNGFr-positive Schwann cell fraction was confirmed by vimentin and S100β double immunofluorescence (Supplementary Figure 1).

2.3. Preparation of nerve guides

Perimaix nerve guides were generated by Matricel GmbH (Herzogenrath, Germany) using a patented uni-directional freezing process [10] (see Supplementary video 1 in [9]). Purified porcine collagen, characterized by low levels of non-collagenous and non-elastin markers, was used as a starting material for the nerve guide (Table 1). The main geometrical requirements for the novel nerve guide were: (1) a cylindrical form with a diameter of 1 mm and a length greater than 2 cm, (2) densely packed, longitudinally orientated microchannels capable of allowing SC adhesion, proliferation and migration as well as axonal growth.

The degree of cross-linking of the nerve guides was related to a decrease in free amine group content and an increase in denaturation temperature. The free amine group content of the samples was determined spectrophotometrically after reaction of the primary amine groups with 2,4,6-trinitrobenzenesulphonic acid (TNBS) as described previously [9]. The free amine group content was expressed as the number of free amine groups present per 1000 amino acids (n/1000 n). The percentage of reacted amine groups was calculated by setting the amine group content of non-crosslinked sample to 100%. The denaturation temperature of the nerve guides was determined by differential scanning calorimetry (DSC) using a TA Instrument Q100. In an empty hermetic pan, approximately 1 mg of scaffold was weighed, followed by the addition of 11 mg phosphate buffered saline solution. The sample was allowed to rehydrate overnight at room temperature before it was scanned at 5 °C/min in the range of 15–95 °C. Excess acid present from the directional solidification process was removed to prevent unwanted pH shifts. The peak temperature was taken as the denaturation temperature.

Fully hydrated samples of the cross-linked, sterilized, and orientated nerve guides were placed between the upper and lower plates (25mm diameter) of a controlled stress rheometer (Rheometrics Scientific, Piscataway, NJ). The oscillation frequency was varied from 0.01 to 20 Hz, and the strain was kept within the linear visco-elastic region for the measurements. The measurements were

Table 1
Characterization of cross-linking of the Perimaix nerve guides. Please note the decrease in denaturation temperature after gamma sterilization, which is a well-known phenomenon for collagen-based biomaterials [11]. In this previous study, the decrease in denaturation temperature resulted in a slightly faster degradation rate. (All measurements were performed $n = 3$, data is presented as mean + standard error of the mean).

Code	Non sterile samples		Sterile samples
	% of free amine groups reacted	Denaturation temperature (°C)	Denaturation temperature (°C)
Perimaix-17%	17	71.1 + 0.3	55.0 + 0.4
Perimaix-33%	33	76.7 + 0.2	60.5 + 0.4

performed at room temperature. Visco-elastic rheometric analysis of fully hydrated (distilled water) comparable sponge structures revealed that the nerve guides were predominantly elastic, with a shear modulus of 4.5 + 1.8 kPa (see also [11]).

In order to achieve parallel oriented ice crystal growth, the collagen suspension was cooled and frozen using a unidirectional freezing process with a defined temperature gradient and a constant cooling rate (Supplementary Figure 2). The temperature gradient was applied between two temperature controlled blocks (warm and cold block) and the collagen sample moved continuously through this temperature field with a constant velocity (v). One block was kept at a constant temperature above the freezing point (T_{warm}) whereas the other one was kept below the freezing point of the suspension (T_{cold}). Thus, steady thermal conditions and an almost one dimensional heat flow (q) in the direction of the temperature gradient were created, leding to a fixed position of the ice front between the two heat sinks. Since the collagen sample was moved through the temperature field, there was the continuous formation of the uniformly structured nerve guide according to the Bridgman process [14]. After freeze-drying of the solidified collagen suspension, the degradation rate of the nerve guides was adapted with a tested degree of cross-linking for peripheral nerve regeneration. This included optimal SC viability and neurite outgrowth from DRG neurons under in-vitro conditions, as described previously [9]. Sterility of the nerve guides was achieved by exposure to 25 kGy ^{60}Co gamma irradiation.

2.4. Seeding of SC into the Perimaix nerve guides

Under sterile conditions, 25 μL of SC suspension (20,000 cells/μL) was pipetted into a petri dish and the Perimaix nerve guide was dropped into the cell suspension (step 1; see Supplementary video 1). After the cell suspension had been fully absorbed into the nerve guide, a further 25 μL SC suspension was pipetted from above (total volume applied = 50 μL). In the case of cell-seeded nerve guides (i.e. groups I, III, and VII–X), the Perimaix nerve guides were loaded with SC 16–24 h before implantation.

Supplementary video related to this article can be found at doi:10.1016/j.biomaterials.2011.10.069

2.5. Confocal laser scanning microscopy (CLSM)

The seeding of Perimaix nerve guides and cell distribution after a cultivation period of 16–24 h (i.e. before implantation in the rat model for PNI) was investigated using confocal laser scanning microscopy (CLSM; Leica TCS SP2 AOBS, Wetzlar Germany) using 488-nm wavelength excitation light. The use of CLSM allowed for assessment of GFP-positive SC (GFP/SC) without any tissue manipulation (such as sectioning and immunohistochemical staining procedures). A sub-set of animals with a sciatic nerve injury (PNI model) was treated with Perimaix nerve guides seeded with GFP/SC. At one week and 6 weeks after implantation, GFP/SC-seeded Perimaix nerve guides were explanted, fixed with 3.9% glutaraldehyde and the presence of GFP/SC was again assessed by CLSM.

2.6. Experimental design and surgery

Adult Lewis inbred rats (Charles River©, Sulzfeld, Germany) weighing approximately 220 g were divided into 10 groups (Table 2), and studied over a period of 6 weeks after nerve injury (i.e. groups I–VI, IX–X) unless indicated otherwise (i.e. groups VII–VIII).

After brief isoflurane sedation (Abbot, Ludwigshafen, Germany), animals were anesthetized by subcutaneous injection with a mixture of medetomidin (Dormitor®, 0.3 mL/kg) and ketamine (10%, 0.6 mL/kg). The right sciatic nerve was exposed by blunt dissection and animals in all groups (except group VI) were subjected to the microsurgical epineurial sheath tube (EST) technique (Fig. 1), as described elsewhere [15,16]. Briefly, the outer epineurium was incised over a length of 2 cm. The nerve fascicles were detached from the outer epineurium in an atraumatic fashion and transected proximally and distally, perpendicular to the longitudinal axis while preserving the integrity of the epineurial tube. Microscopic inspection was used to ensure that no residual sciatic nerve fascicles remained in the emptied epineurial tube and that the epineurium had not become twisted or damaged. Perimaix nerve guides were placed into the epineurial tube to bridge the proximal and distal sciatic nerve stumps in such a way that the implant abutted both nerve stumps. The epineurial tube was then closed using tensionless single stitches with 10-0 monofilament nylon (Ethilon®, Ethicon Inc, Somerville, USA) (Fig. 1). Parallel control experiments with histological examination (transverse sections stained with toluidine blue [see below]) confirmed that no residual nerve fibres were left in the epineurial tube (Fig. 1d). Additional sirius red stainings confirmed these findings (Fig. 1E–F). For this purpose, tissue samples were kept in formalin 10% solution for 24 h and stored at 4 °C. They were embedded in paraffin and mounted on sialinized plates. 5μm sections were stained for 1 h in picrosirius solution (0.1% solution of Sirius Red F3BA in saturated aqueous picric acid, pH 2) [17,18].

Table 2
Experimental groups.

Groups	Material	Functionalization	Abbreviation	Time
I ($n = 7$)	Perimaix-17%	With SC	PM-17 [+SC]	6 weeks
II ($n = 7$)	Perimaix-17%	Without SC	PM-17 [−SC]	6 weeks
III ($n = 7$)	Perimaix-33%	With SC	PM-33 [+SC]	6 weeks
IV ($n = 7$)	Perimaix-33%	Without SC	PM-33 [−SC]	6 weeks
V ($n = 7$)	Fibrin (control)	–	Fibrin [−SC]	6 weeks
VI ($n = 7$)	Autologous nerve (control)	–	ANT	6 weeks
VII ($n = 4$)	Perimaix-17%	With GFP-positive SC	PM-17 [+GFP/SC]	1 week
VIII ($n = 4$)	Perimaix-33%	With GFP-positive SC	PM-33 [+GFP/SC]	1 week
IX ($n = 2$)	Perimaix-17%	With GFP-positive SC	PM-17 [+GFP/SC]	6 weeks
X ($n = 2$)	Perimaix-33%	With GFP-positive SC	PM-33 [+GFP/SC]	6 weeks

Animals in group V served as a 'negative control group'. Commercially available fibrin glue (Tissucol Duo S®; Baxter, Vienna, Austria) was used to produce fibrin cylinders (dimensions: 1 mm in diameter and 2 cm in length) with the aid of a sterilizable teflon-coated block with multiple longitudinal grooves (see Supplementary Figure 3). The longitudinal grooves were filled with the fluid fibrin glue. After polymerisation, these pliable fibrin cylinders were inserted into the empty epineurial tube following the same procedure as described above [10]. The fibrin cylinders had two main advantages: firstly, they were free of cells or any kind of growth factors; secondly, they were biocompatible and prevented collapsing after suturing of the outer epineurium (Fig. 1C–F).

Animals in group VI served as a 'positive control group'. Here, an autologous nerve was used to bridge the sciatic nerve defect. Briefly, the right sciatic nerve was completely excised proximally and distally over a distance of 2 cm. The excised nerve segment was removed and immediately re-implanted using 4x epineurial single monofilament polyamide stitches (10-0 Ethilon, Ethicon Inc., Somerville, USA). For further details see [16,19].

2.7. Histomorphometry and electron microscopy

With the exception of animals from groups VII and VIII, rats were euthanized after a period of 6 weeks. The sciatic nerves were dissected, mounted on a cork plate and immersion fixed for 24 h in 3.9% glutaraldehyde. A 1–2 mm slice of the regenerated nerve was taken at the distal end of the implant. These nerve samples were osmicated, dehydrated and embedded in Epon. Transverse semi-thin sections (1μm thick) were stained with toluidine blue for morphometric analysis, while ultra-thin sections (50nm) were used for transmission electron microscopy (TEM) as described previously [20]. Nerve guides were also processed for scanning electron microscopy (SEM). Samples were fixed in 4% glutaraldehyde in 0.1 M PBS (24 h), dehydrated in acetone using a Polaron E3000 critical point dryer (Polaron Equipment Ltd., Watford, United Kingdom), mounted on stubs and sputter coated with gold. Samples were then loaded into an ESEM XL30 FEG scanning electron microscope (Philips EO, Eindhoven, NL) and viewed under an accelerating voltage of 5 kV.

Morphometric evaluation was performed using a computer-assisted system based on Zeiss KS 300 2.0 software (Axon_100.mcr, www.zeiss.de/imaging, Zeiss, Oberkochen, Germany) in combination with a microscope (Axioskop, Zeiss, Germany) equipped with a colour camera (Prog/Res/3008, Kontron AG, Munich, Germany). The data from all groups were assessed in a blinded manner. Nerve fibre density and axon diameter/myelin thickness [21] were determined in 5 randomized fields of interest (FOI; area: 1530μm^2) from the entire cross-section of the sample. Axon g-ratios (i.e. the ratio of axon diameter to total fibre diameter) were also determined (a value of 0.6–0.7 is detectable in intact nerves [19]).

2.8. Data presentation and statistical analysis

Data are expressed as mean +/− standard-error-of-the-mean (sem). Statistical analysis included analysis of variance (ANOVA) with Tukey *post hoc* correction to correct for multiple comparisons. A *p*-value of 0.05 was regarded as statistically significant.

3. Results

3.1. Nerve guides

PM-17 and PM-33 nerve guides, 4 cm long and 1 mm diameter, were designed for the experiments. Scanning electron microscopy (SEM) demonstrated the longitudinally orientated micro-channels (mean diameter of 50 μm) that were continuous from one end to the other. The channels were interconnected and stabilized via single strands of collagen that were usually perpendicular to the longitudinal axis (Fig. 2A–B). The extensive porosity of the micro-channel walls facilitates diffusion within the scaffold (i.e. delivery of nutrients and removal of metabolites) and the homogeneity of SC

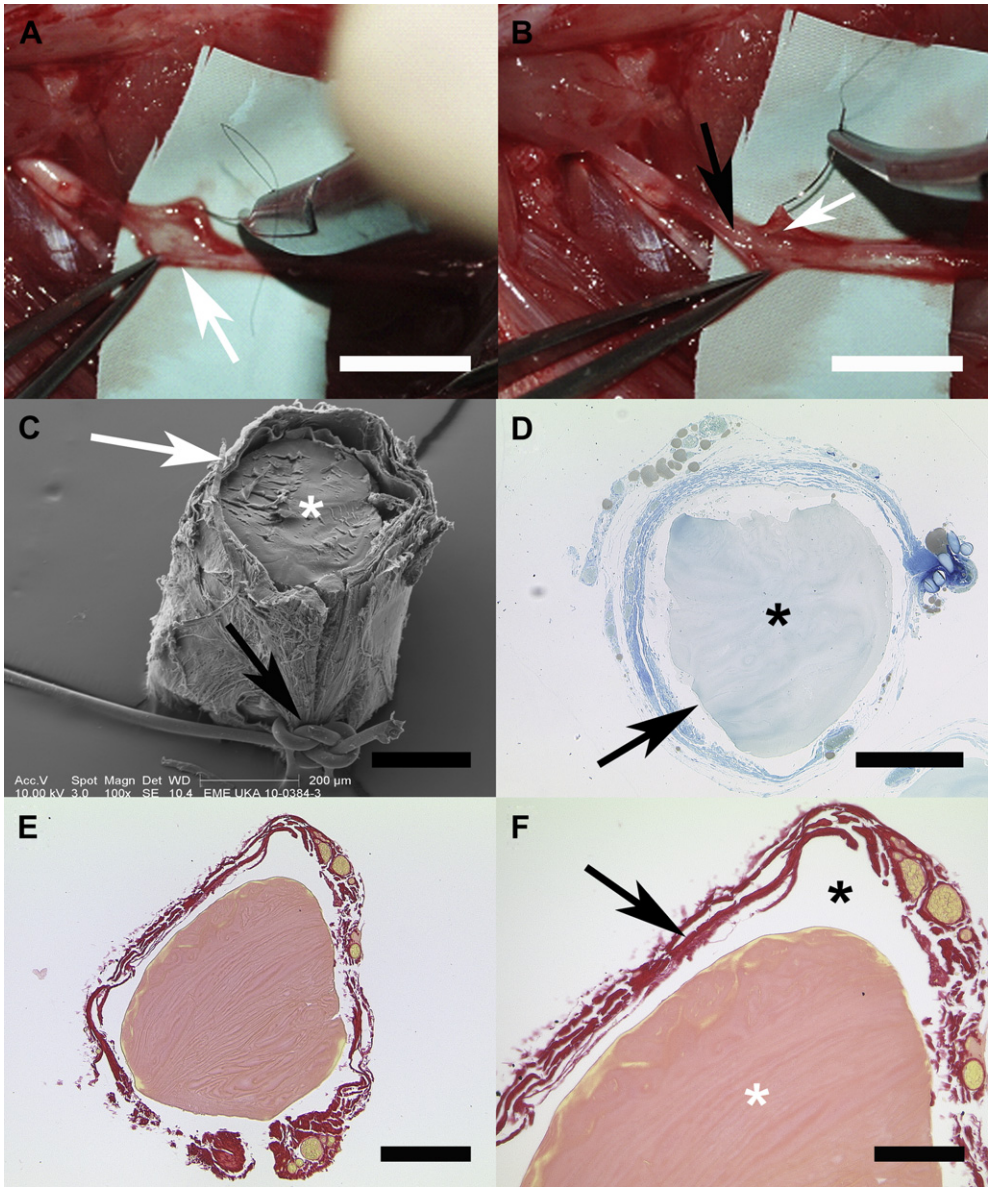

Fig. 1. The epineural sheath tube (EST-) technique. After incision of the outer epineurium and resection of the nerve fascicles, the preserved epineural tube has no macroscopical residua of nerve fibres (white arrow in A). Note the implanted nerve guide (black arrow in B) in the prepared epineural tube (white arrow in B). Representative samples (C–F) from additional animals (not included in group V) were prepared and examined directly after surgery. A scanning electron micrograph of a fibrin glue cylinder (white asterisk in C) within the epineural tube (white arrow in C) which has been closed by tensionless single stitches with 10-0 monofilament nylon (black arrow in C). Transverse semi-thin section of the implanted fibrin gel stained with toluidine blue (D) or sirius red staining (E,F). Note the fibrin glue cylinder (black asterisk in D and white asterisk in F). High magnification microscopy confirmed the lack of any residual nerve fibres in the EST technique (black arrow in D and black asterisk in F). Scale bars: A-B = 1 cm, C-E = 200 µm, *F* = 100 µm. (For interpretation of the references to colour in this figure legend, the reader is referred to the web version of this article.)

loading [9]. The nerve guides were highly hydrophilic and demonstrated rapid fluid absorption, as seen during cell seeding with the SC suspension (Supplementary video 1). The nerve guides did not swell and retained their structural integrity after wetting (Fig. 2A–B).

3.2. Schwann cells

Samples of GFP/SC and GFP-negative SC cultures were characterized by vimentin and S100β double immunofluorescence. The populations were highly enriched with SC displaying a typical, spindle-shaped, bipolar (sometimes tripolar) morphology (Supplementary Figure 1). Confocal microscopy demonstrated the adhesion and distribution of GFP/SC, 16-24h after seeding into the nerve guides (Fig. 3). Donor cells showed a near homogeneous distribution throughout the porous nerve guides, aligning themselves and their processes along the longitudinal axis of the micro-channels (white arrows in Figs. 3 and 4; see also Supplementary videos 2 and 3).

Supplementary video related to this article can be found at doi: 10.1016/j.biomaterials.2011.10.069

Supplementary video related to this article can be found at doi: 10.1016/j.biomaterials.2011.10.069

Donor SC were also still clearly viable at 1 week (Figs. 4; see Supplementary video 3) and 6 weeks (Fig. 5) after implantation (white arrows in Figs. 4 and 5). The aligned SC within the longitudinal micro-channels resembled Bands of Büngner (e.g. red arrow, Fig. 4B; see also Supplementary video 3).

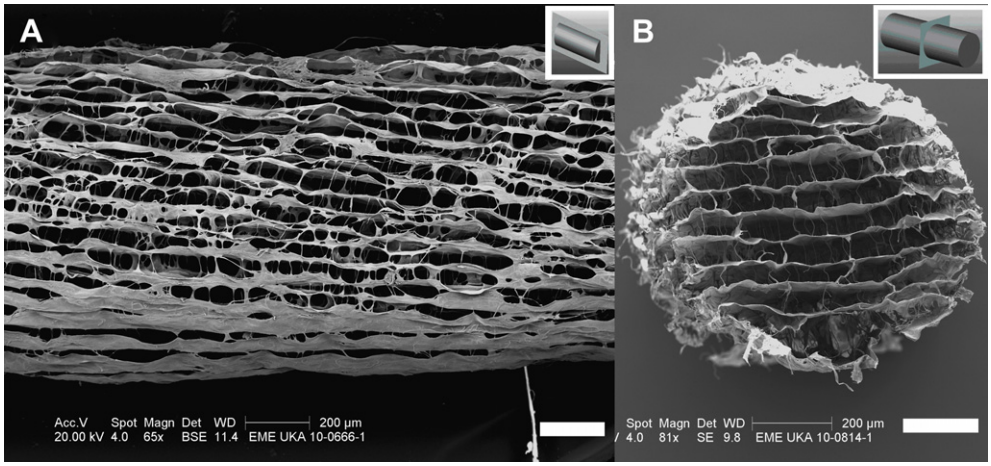

Fig. 2. Perimaix nerve guides. A SEM of the longitudinal microstructure of the Perimaix nerve guide. B: SEM of the transverse microstructure (average pore diameter being approximately 50 µm). Scale bars: A-B = 200 µm.

3.3. General observations following nerve guide grafting

All animals recovered well from the surgery, as revealed by a steady increase in body weight (data not shown). Importantly, there were no signs of autotomy (i.e. automutilation behaviour) throughout the study period. Explanted Perimaix nerve guides appeared well-integrated with the host tissue (groups I–VI) and showed no obvious macroscopic signs of inflammation, dislocation or neuroma formation. In group II (PM-17 [−SC]), group IV (PM-33 [−SC]) and, in particular, group V (fibrin [−SC]) the sciatic nerves were relatively thin. In contrast, implants from groups I (PM-17 [+SC]), III (PM-33 [+SC]) and VI (ANT) were apparently of normal thickness and well vascularised (Fig. 6).

3.4. Light-microscopic observations

Histology revealed an excellent toleration of the Perimaix nerve guides with no indication of inflammatory or foreign body reactions (Figs. 7 and 8). Residues of the collagen nerve guides could only be observed in animal groups receiving non-seeded implants (i.e. groups II and IV; see also Fig. 9). In contrast, the collagen nerve guide was replaced by neural tissue (e.g. perineurium-like connective tissue elements and myelinated axons) in groups receiving SC-seeded nerve guides (groups I and III; Figs. 7 and 8). In the negative controls (group V, fibrin [−SC]), the distal part of the graft was devoid of axons (data not shown). This observation was important to prove that axon regeneration in groups I–IV was due to the Perimaix nerve guide rather than any intrinsic property of the epineurial tube. Qualitatively, cross sections showed groups of 15–20 myelinated axons which were arranged in bundles (e.g. Figs. 7 and 10), surrounded by a thin connective tissue layer containing perineurial-like cells (e.g. black arrows, Fig. 10). The longitudinal sections revealed groups of axially arranged nerve fibres and their nodes of Ranvier (see white arrow in Fig. 8D).

3.5. Transmission electron microscopical (TEM) observations

The fascicular pattern of regenerating axons within the nerve guide was also observed by TEM. In all groups where axon regeneration could be demonstrated, the mini-fascicles were characterized by small numbers (approximately 10–20) of myelinated axons, which were surrounded by a new perineurium (black arrows in Fig. 10). The diameter of the mini-fascicles often corresponded with the diameter of the original pore channels (~50 µm).

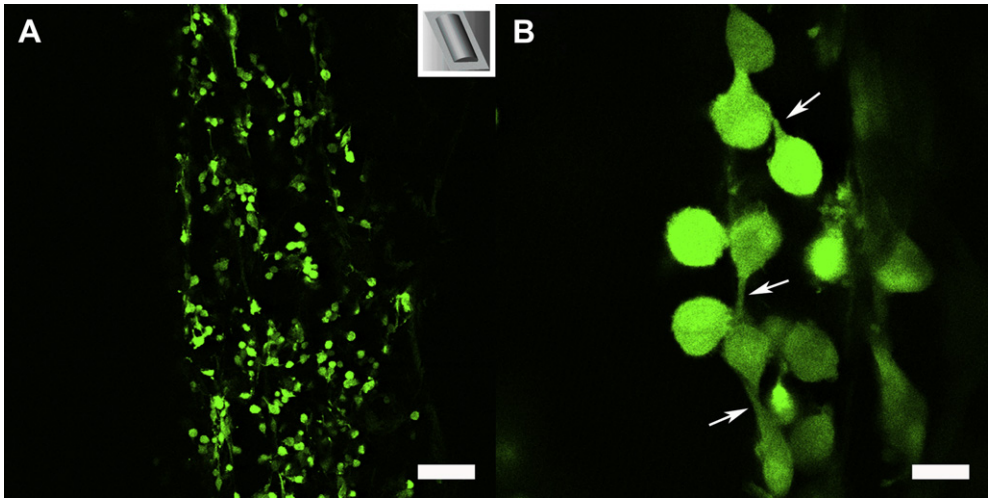

Fig. 3. CLSM of GFP/SC seeded into the Perimaix nerve guide prior to implantation. A: Low magnification longitudinal image demonstrating the dense and near homogeneous seeding of SC into the nerve guide (group VII: PM-17 [+GFP/SC]). B: Higher magnification of A showing rounded SC bodies and processes extension (see white arrows) that followed the orientation of nerve guide's microstructure. Scale bars: A = 200 µm, B = 20 µm.

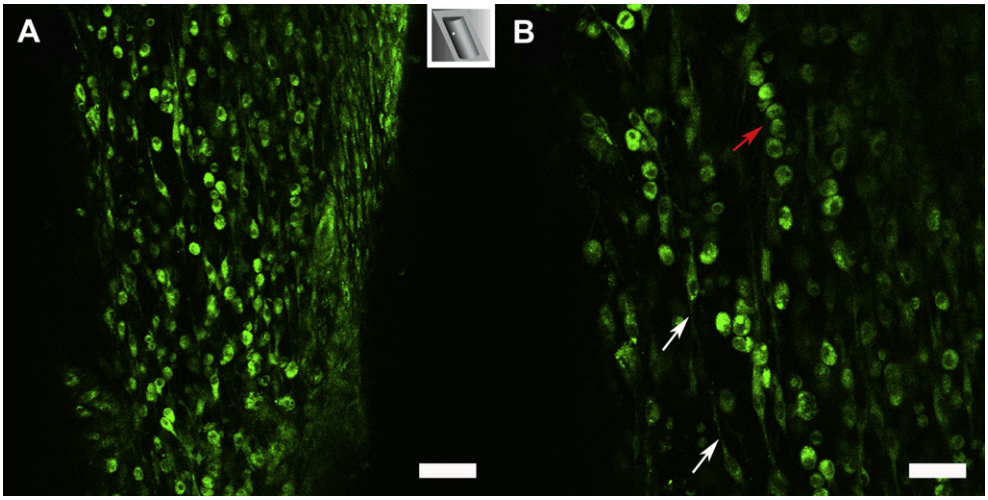

Fig. 4. CLSM of GFP/SC seeded nerve guide 1 week after implantation into a sciatic nerve defect (group VII: PM-17 [+GFP/SC]). A: Low magnification, image showing the maintained dense and near homogenous packing of donor cells within the nerve guide. B: Higher magnification demonstrating round and oval cell bodies with long, fine processes (white arrows). Cell bodies often appeared to be aligned or packed as orientated columns, resembling "bands of Büngner" (red arrows). Scale bars: A = 100μm, *B* = 50 μm. (For interpretation of the references to colour in this figure legend, the reader is referred to the web version of this article.)

3.6. Quantitative morphometric analysis

In the positive controls (group VI, ANT), axons with a typical regenerative morphology were observed (Figs. 7 and 8). Morphometric analysis of axons revealed a myelinated axon density of 200 ± 13 per FOI (i.e. per 1530 μm^2), a mean axon diameter of 1.0 ± 0.04 μm, and a mean myelin thickness of 0.3 ± 0.01 μm. In the experimental groups, a clear difference could be observed between SC-seeded Perimaix nerve guides and cell-free Perimaix nerve guides. Four out of 7 of the non-seeded nerve guides displayed disseminated axons in the distal part of the graft, with an average axon density that was significantly lower than in the SC–seeded nerve guides, i.e. 40 ± 11 and 89 ± 28 per FOI in groups II and IV, respectively (Fig. 11A). However, the mean axon diameter and the mean diameter of myelinated axons did not differ significantly from that of the ANT group (Fig. 11B,E). Myelin thickness, in contrast, was significantly lower in the two non-seeded Perimaix groups (mean values of 0.2 ± 0.02 μm in both groups) than in the ANT group (Fig. 11C).

Cell-seeding of Perimaix nerve guides generally improved axon regeneration, since the results obtained were often similar to those observed in the ANT group. Indeed, the mean axon density of group I (i.e. PM-17 [+SC]) was not significantly different from that of group VI (i.e. ANT), with values of 174 ± 14 and 200 ± 13 per FOI, respectively (Fig. 11A). Furthermore, the mean thickness of the myelin sheaths was not different between groups I and VI (0.3 ± 0.01 μm in both groups; Fig. 11C). The values observed in group III (i.e. PM-33 [+SC]) were slightly lower; average axon density per FOI (132 ± 18) and the mean myelin thickness (0.2 ± 0.01 μm) (Fig. 11A,C).

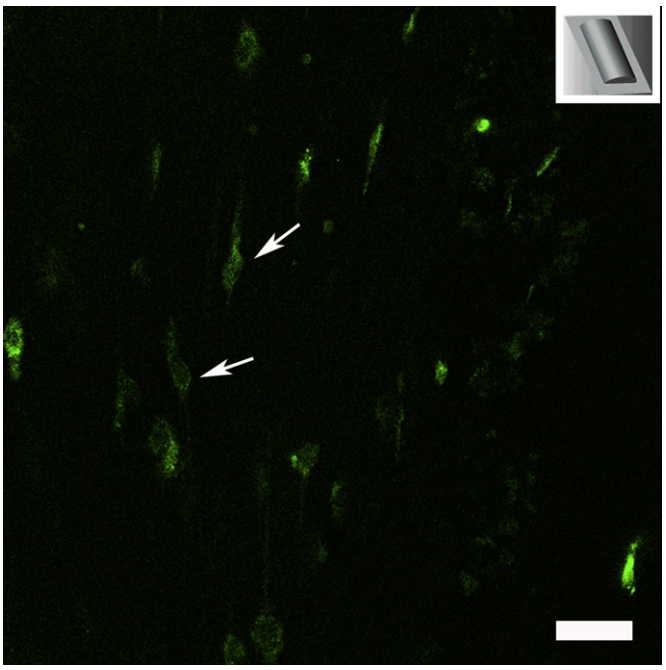

Fig. 5. CLSM of GFP/SC seeded nerve guide 6 week after implantation into a sciatic nerve defect (group VII: PM-17 [+GFP/SC]). Bipolar GFP/SC are still detectable in the regenerated nerve (white arrows). Scale bar: 50 μm.

4. Discussion

At present, the transplantation of autologous nerves still provides the best clinical substrate for axon regeneration in the repair of nerve defects (clinical "gold standard") [3,22]. However, only 40–50% of patients regain useful function when treated with ANT [5]. The main goal of the present research was to develop a biomimetic scaffold with a 'regenerative performance' that matches or even surpasses the results of ANT. Sophisticated strategies in the development of customized nerve guides are expected to yield superior results (e.g [23–27]).

The biomimicking concept, as presented in the current study and discussed by other researchers [3,6,7,28] suggests that the therapeutic value of a nerve guide could depend on the close matching of the physical and biochemical properties of a peripheral nerve. However, it must be noted that this is only one option. There are a number of concepts which do not employ typical "biomimetic" nerve guides (e.g. without SC enrichment, without ECM components etc.) but still achieve good results in bridging long nerve defects (e.g. [23,24]). In this context, the biomimicking concept has also been adopted for the central nervous system. Teng and colleagues [8] designed a two-component polymer scaffold

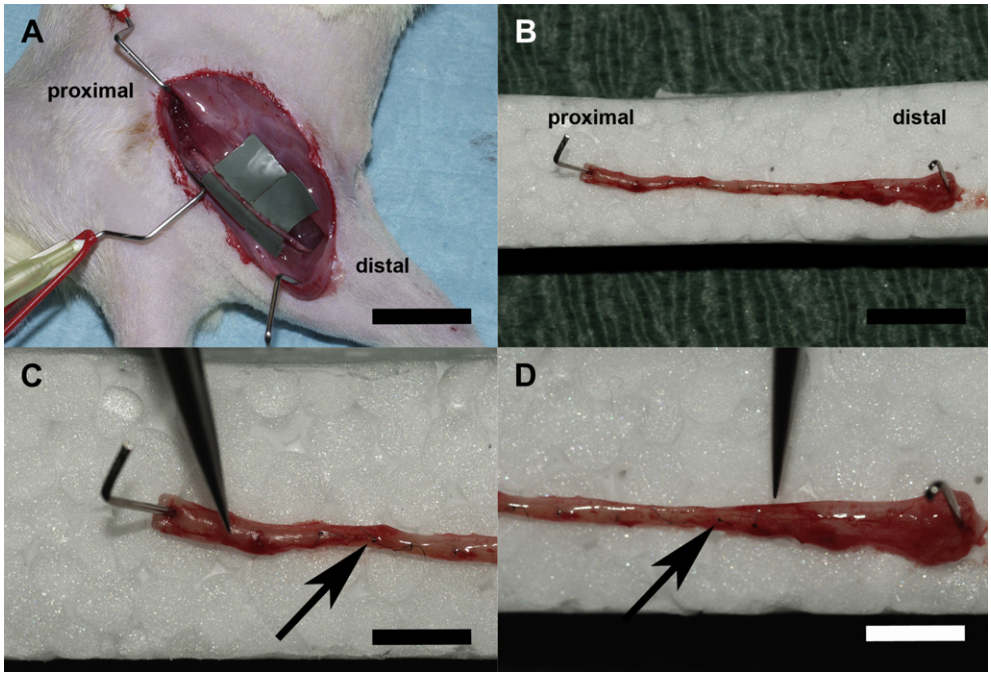

Fig. 6. Sciatic nerve graft site at 6 weeks following implantation (PM-17 [+SC]). (A) Macroscopic view *in situ* and (B) after explantation and fixation onto a polystyrene support. (C–D) Note the magnified proximal and distal ends (respectively) of the nerve guide (indicated by the tip of the scissors). Scale bars: A = 2 cm, B = 1 cm, *C* = 0.5 cm, *D* = 0.25 cm.

that simulated the architecture of the healthy spinal cord. The scaffold's internalportion mimicks the grey matter using a porous polymer layer (seeded with neural stem cells). The outer portion of the scaffold emulated the white matter with longitudinal pores for guided axonal growth [8].

In the present study, two scaffold prototypes, which differ in their chemical properties (Table 1), were found to be highly permissive and allowed for infiltration of tissue cultured SC. This resulted in the indirect 'functionalization' of the nerve guides, since SC produce a large repertoire of biochemical factors known to support axon regeneration [28,29]. The donor SC showed excellent adherence to nerve guide prototypes, as reported previously [9].

The hydrophilic properties of the nerve guides allowed for rapid fluid uptake [Supplementary video 1]. The hydrated nerve guides remained their structural integrity and showed no signs of collapse, supporting earlier *in-vitro* studies [11]. This is an important prerequisite for achieving successful nerve regeneration. The loss of its structural integrity before completion of axonal regeneration can be detrimental for the regenerative properties of a nerve guide. This open and longitudinally orientated microstructure of the Perimaix nerve guides provided the framework for directed glial cell migration and axonal growth *in vivo*. The current investigation confirmed the regenerative potential of the Perimaix nerve scaffolds, and expands on previous relatively simple short term *in vitro* investigations [9,11].

Most experimental approaches in bridging peripheral nerve defects have employed hollow tubes. However, there is growing evidence that the lumen of these devices requires axon growth promoting substrates which is essential for bridging large nerve gaps [3,7]. The Perimaix collagen-based nerve guides mimic some of the natural topographical features of normal peripheral nerves. The micro-structured nerve guide contains numerous longitudinally orientated channels with cross-sections of approximately 50 μm in diameter [9–11]. Importantly, SC were also found to form cellular bundles within the pore channels of the Perimaix nerve guide, which were reminiscent of the so-called 'bands of Büngner'. The latter bands form an important basis of successful axon regeneration [30,31].

The use of SC isolated from transgenic GFP rats allowed the detection and monitoring of transplanted cells at 1 and 6 weeks post implantation. The use of GFP expression by donor cells is superior to other cell tracking techniques including labelling with BrdU, Fast blue, or DAPI. These methods are limited by dilution of signalling resulting in continued proliferation or label leakage [32–35].

In the current study, the regenerative properties of PM-17 and PM33 in an experimental model of peripheral nerve injury have been tested. Implantation of SC-loaded Perimaix nerve guides into the 2 cm defects in the rat sciatic nerve was found to support axon regeneration at 6 weeks post implantation. This experimental study design with a gap size of 2 cm and a regeneration period of 6 weeks represents a challenge for PNS repair. The 2 cm gap is regarded as being significantly larger than the critical defect size in the adult rat [36]. However, a survival period of 6 weeks may be regarded as insufficient to allow for complete functional repair, well noting that axon regeneration through ANT takes place at approximately 1–2 mm per day [3]. The SC-seeded PM-17 nerve guide was found to be almost as effective as the gold standard ANT with respect to the density of regenerated axons, axon diameters and axon myelinization (Figs. 7 and 8, 11). Although the non-seeded Perimaix scaffolds also supported axon regeneration, this effect was inferior to the SC-seeded scaffolds (Figs. 9 and 11).

As central part of the biomimicking concept, the use of collagen as the basis for the Perimaix nerve guide offers many advantages. Collagen, as an ubiquitous extracellular matrix protein, plays a key role in the formation of nerve connective tissue matrix. One key feature is that the degradation rate could be adjusted by the degree of cross-linking. In previous studies, the degree of cross-linking of Perimaix scaffolds (Table 1) had no significant adverse effects on SC viability [9]. It might be possible to customize the extent of cross-linking depending on the dimensions of the nerve defect. Larger

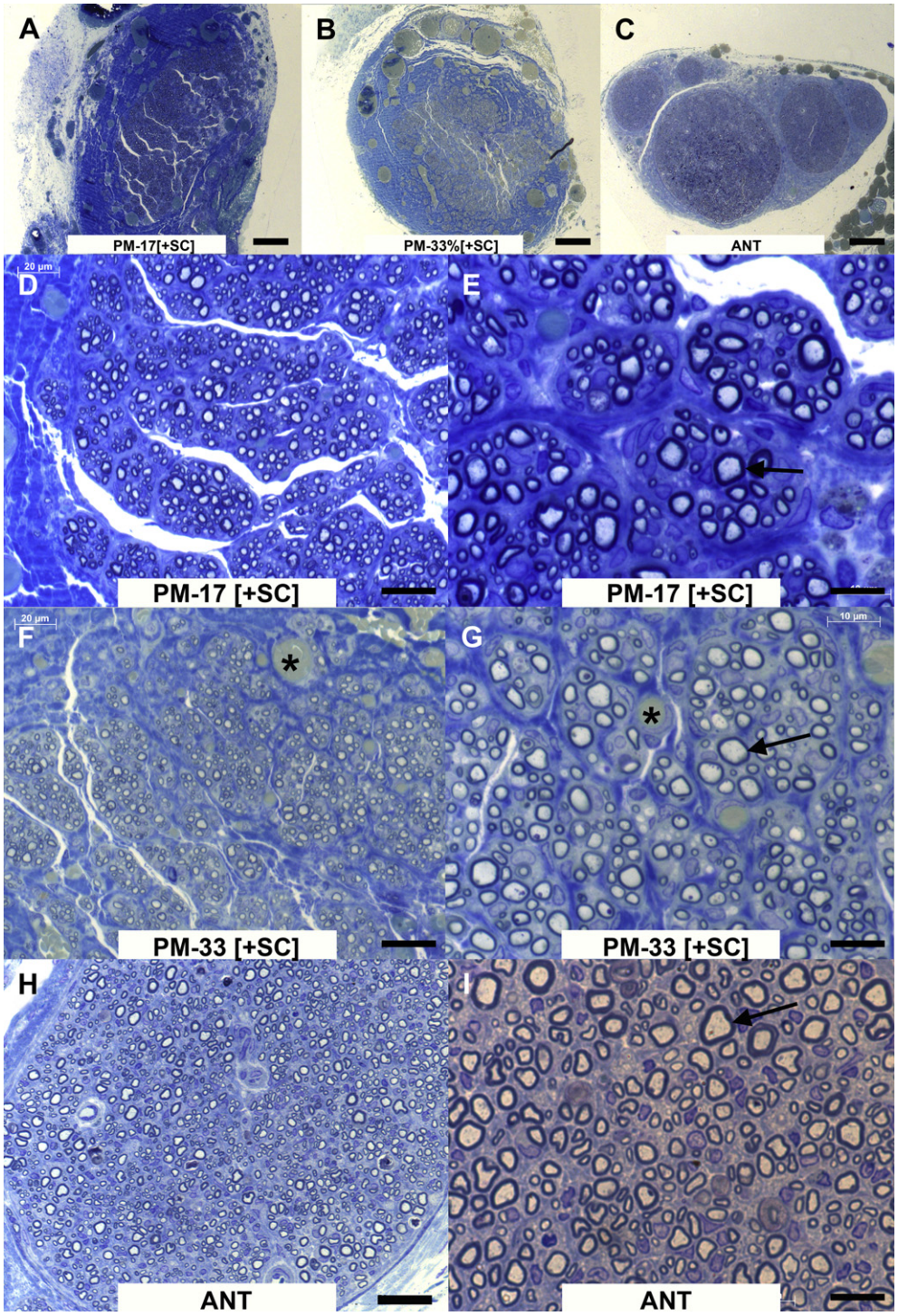

Fig. 7. Cross-sections of the distal part of the various grafts at 6 weeks after implantation. Semi-thin sections were stained with toluidine blue. A, D–E: PM-17 [+SC], B, F–G: PM-33 [+SC], C, H-I: ANT. Note the arrangement of regenerated (myelinated) axons in bundles or mini-fascicles. Myelinated axons are indicated by black arrows and congested blood vessels filled with erythrocytes are indicated by black asterisks. Scale bars: A–C = 100 µm, D, F, H = 20 µm, E, G, D = 10 µm.

gaps may require a higher degree of scaffold cross-linking, and thus a lower degradation rate, since regeneration across large defects takes longer and requires a prolonged maintenance of implant architecture. However, this aspect of scaffold refinement requires further investigation.

According to Schmidt & Leach [28] and others, an "ideal" nerve guide consists of a biodegradable porous conduit with intraluminal guidance for orientated nerve growth and enrichment with support cells or growth factors. Bridging peripheral nerve gaps has been studied in a large number of in-vitro and in-vivo studies. However, there are two main reasons why the generated data and the efficacy cannot be directly compared.

First, these studies employed different strategies to repair damaged nerve tissue. The concepts mainly differed in the choice

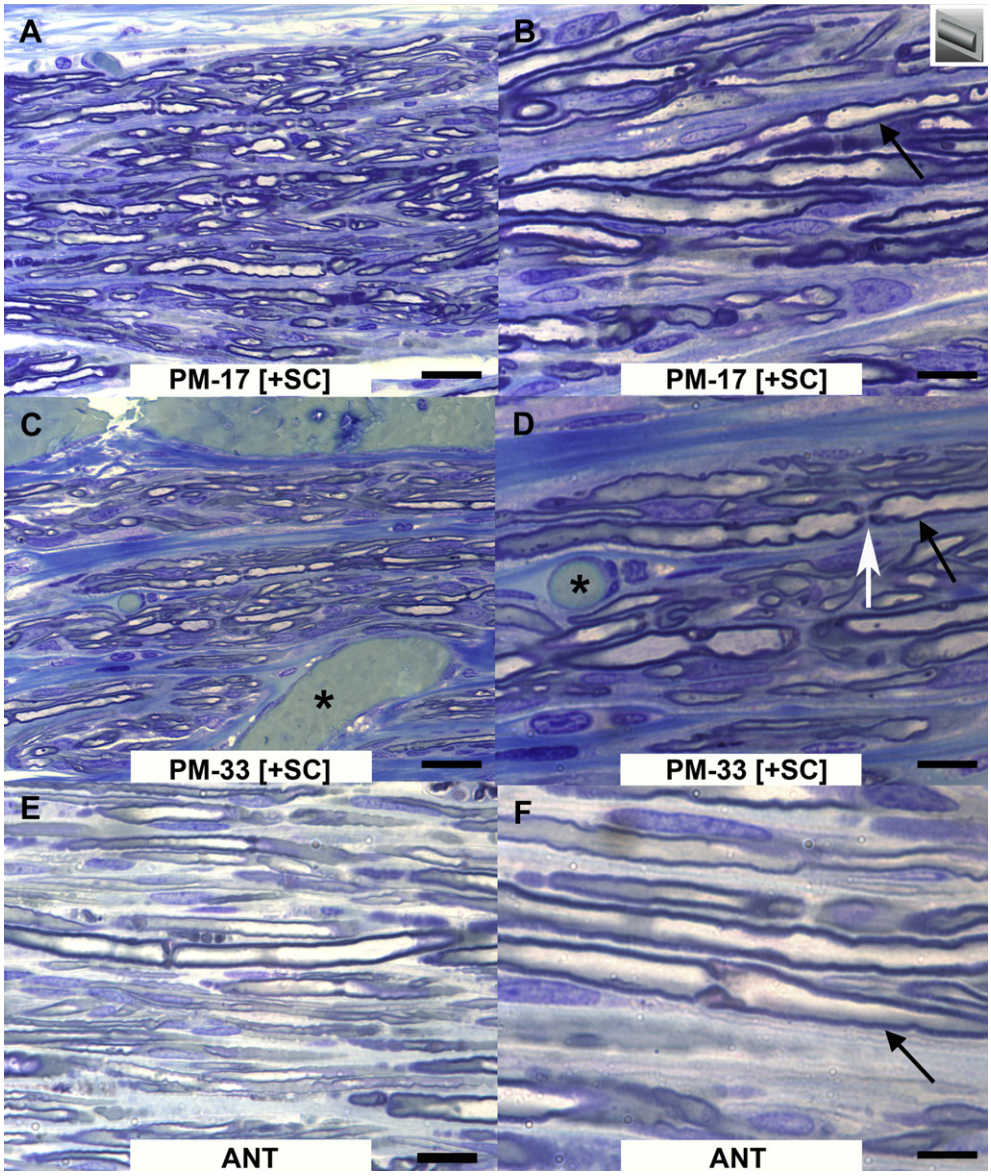

Fig. 8. Longitudinal sections of the distal part of the various grafts at 6 weeks after implantation. Semi-thin longitudinal sections were stained with toluidine blue. A, B: PM-17 [+SC]. C, D: PM-33 [+SC]. E, F: ANT. Note the orientated growth of myelinated axons (black arrows) with nodes of Ranvier (e.g. white arrow in D). Congested blood vessels (veins, arterioles and capillaries) filled with erythrocytes appear green-turquoise in the toluidine blue-stained sections (black asterisks). Scale bars: A, C, E = 20 μm, B, D, F = 10 μm. (For interpretation of the references to colour in this figure legend, the reader is referred to the web version of this article.)

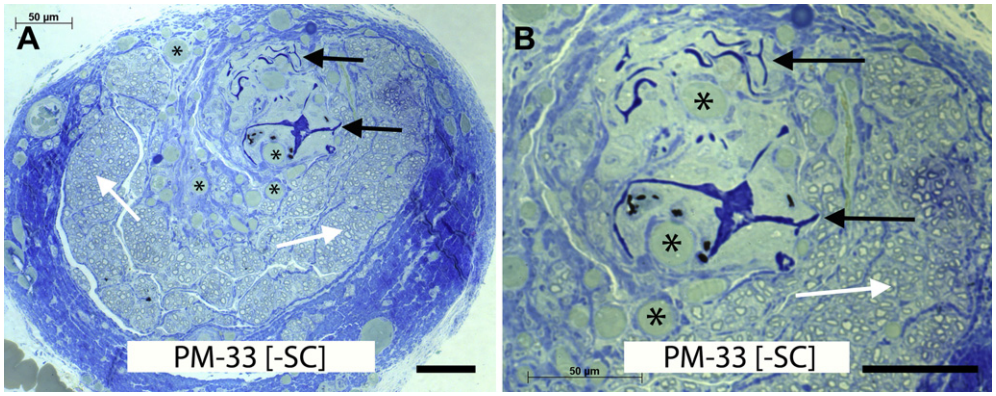

Fig. 9. Cross-sections of the distal part of the PM-33 [−SC] nerve guide (group IV) at 6 weeks after implantation. This example shows that residues of the collagen nerve guides could be observed in groups receiving non-seeded nerve guides. Areas of non-degraded collagen (black arrows) are clearly evident next to areas of myelinated axons (white arrows). Scale bars: A–B = 50 μm.

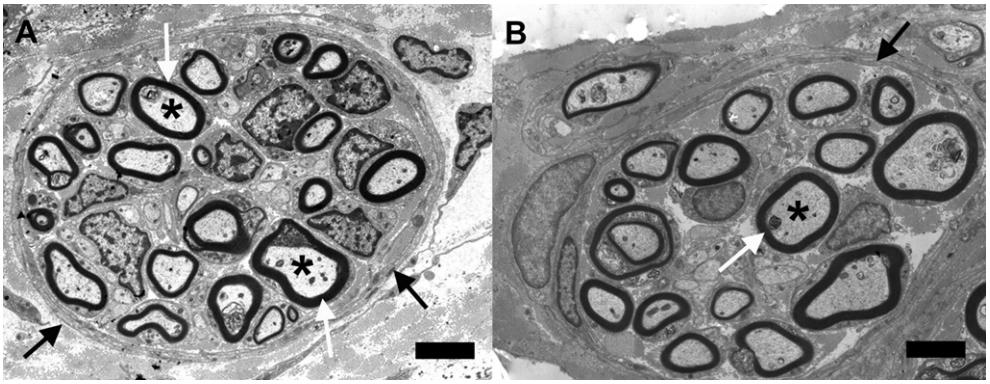

Fig. 10. Transmission electron microscopy of axon regeneration within the Perimaix nerve guides. A: PM-17 [+SC], B: PM-33 [+SC]. Regenerated nerve fibers with a typical morphological features. The mini-fascicles of regenerating axons were enclosed or surrounded by a connective tissue sheath composed of perineurial-like cells (black arrows). These mini-fascicles contained medium-to-large diameter axons (black asterisks) that were surrounded by a myelin sheath (white arrows). Scale bars: A-B = 7 μm.

of a) scaffold materials (e.g. biologic or synthetic, absorbable or non-absorbable etc.), b) geometrical design (e.g. hollow or filled lumen with filaments, fibres, channels, pores etc.), c) cellular or molecular components (e.g. cells or growth factors etc.) [28,37,38].

Second, there is a significant lack of standardization for experimental conditions and assays [36]. This includes the use of (a) different animal species (e.g. rabbit, rat, mouse), (b) nerve models (sciatic -/median-/facial nerve), (c) type of nerve lesions (crushed, hemisected or fully transected nerves), (d) gap length, (e) observation period, and f) assays employed to evaluate the results (histology, electrophysiology, behavioural tests) etc. A comprehensive review has been published by Vleggeert–Lankamp [39]. On the basis of a systematic PubMed research (January 1975–December 2004), studies of sciatic nerve grafting in the rat were considered. The graft had to be composed of synthetic materials; papers describing nerve regeneration through veins, arteries, muscles, or Schwann cell–filled nerve grafts were therefore excluded. Likewise, studies in which a systemic treatment was applied in the rat (e.g. systemic administration of drugs or radiation) were excluded. Further exclusion criteria was the use other animals than rats (e.g. rabbit, mouse), other nerve models than the sciatic nerve (e.g. facial or median nerve), and a gap length shorter than 5mm. Only 31 studies could be extracted examining nerve morphology (e.g. diameter, density and G-ratio) (see Table 3 in [39]). Only one article had a comparable gap length (20mm) as used in our study. Most of the studies had a gap size of 10 mm (15 out of 31) or less (9 out of 31). Furthermore, only two studies had a similar observation period of 6 weeks. One of these studies compared a silicone tube filled with gelatin or collagen gel [40], but only with a gap size of 10mm. The other study [41] tested the effect of controlled NGF delivery in a 13mm gap model. However, most of the cited studies allowed a longer observation period for bridging a nerve gap, ranging from 10 to 60 weeks (22 out of 31). Therefore, a direct comparison of regenerative results between different studies was only limited (see also [36]). This review covered an observation period until the year 2005. Since then a number of experimental studies on SC enriched collagen-based nerve guides with different geometrical characteristics were published. For example, Keilhoff et al. [42] investigated the biocompatibility of a porcine collagen type I/III nerve conduit. After 1 and 2 weeks, nerve guides were harvested and the viability of implanted SC at the inner surface of their hollow collagen conduit was assessed by fluoresceine fluorescence. They demonstrated that implanted SC adhered, survived and were able to form nerve guiding columns of Büngner. This is in agreement with our observations. We could also detect orientated columns of SC resembling “Bands of Büngner” 1 week after implantation (Fig. 4). In addition, we could detect viable SC even 6 weeks after implantation (Fig. 5). In a subsequent study, the same group tested the regenerative capacity of their collagen I/III nerve conduit in a 2 cm rat sciatic nerve gap model [43]. Different variations in the geometrical design were tested (hollow versus inner collagen skeleton, different inner diameters). Their main finding was that nerve regeneration took place in a noteworthy quality with hollow collagen tubes as well as tubes with reduced lumen, both filled with SC. The inner skeleton, however, impaired nerve regeneration independent of whether SC were added or not. They concluded that both viable SC and structural parameters were an imperative prerequisite. This is in accordance with previous publications [6,7,28] and with our own observations. It is important that the geometrical design of an inner skeleton or matrix serves as guidance rather than as a physical blockade impairing axonal growth. The geometrical design was key for the development of our Perimaix nerve guide. The porosity of the micro-channel should facilitate diffusion within the scaffold maintaining SC viability without leading to a collapse of the channels. Therefore, the single strands of collagen perpendicular to the longitudinal axis (Fig. 2A–B) played an essential role in the practicability and effectiveness of our model. The single strands stabilized the pore channels and prevented it from collapsing. This was demonstrated in previous in-vitro studies [9,10], but also in this in-vivo study. For example, TEM observations revealed mini-fascicles with diameters that corresponded with the diameter of the original pore channels (~50 μm; Fig. 10). This indirectly indicated that the pore size remained stable over the regeneration process.

Another study by Yao et al. [44] investigated whether multi-channel nerve conduits may present a permissive microenvironment for axonal growth. They postulated that axons regeneration across single channel tubes may disperse and can result in inappropriate target re-innervation [45]. This dispersion could potentially be limited by multi-channel nerve conduits resembling a nerve’s multiple basal lamina tube. Therefore, Yao and colleagues developed a sophisticated 2-/4-/or 7-channel collagen-based nerve guide with channel diameters ranging from 410 to 530 μm using a 1 cm gap over 24 weeks [44]. They demonstrated the influence of multi-channel guidance on limiting axonal dispersion without decreasing quantitative results of regeneration. This conclusion is in agreement with our concept, since we also tried to mimick the endoneurial basal lamina tubes for orientated nerve growth. Toluidinblue staining of longitudinal sections revealed orientated nerve growth with groups of axially arranged nerve

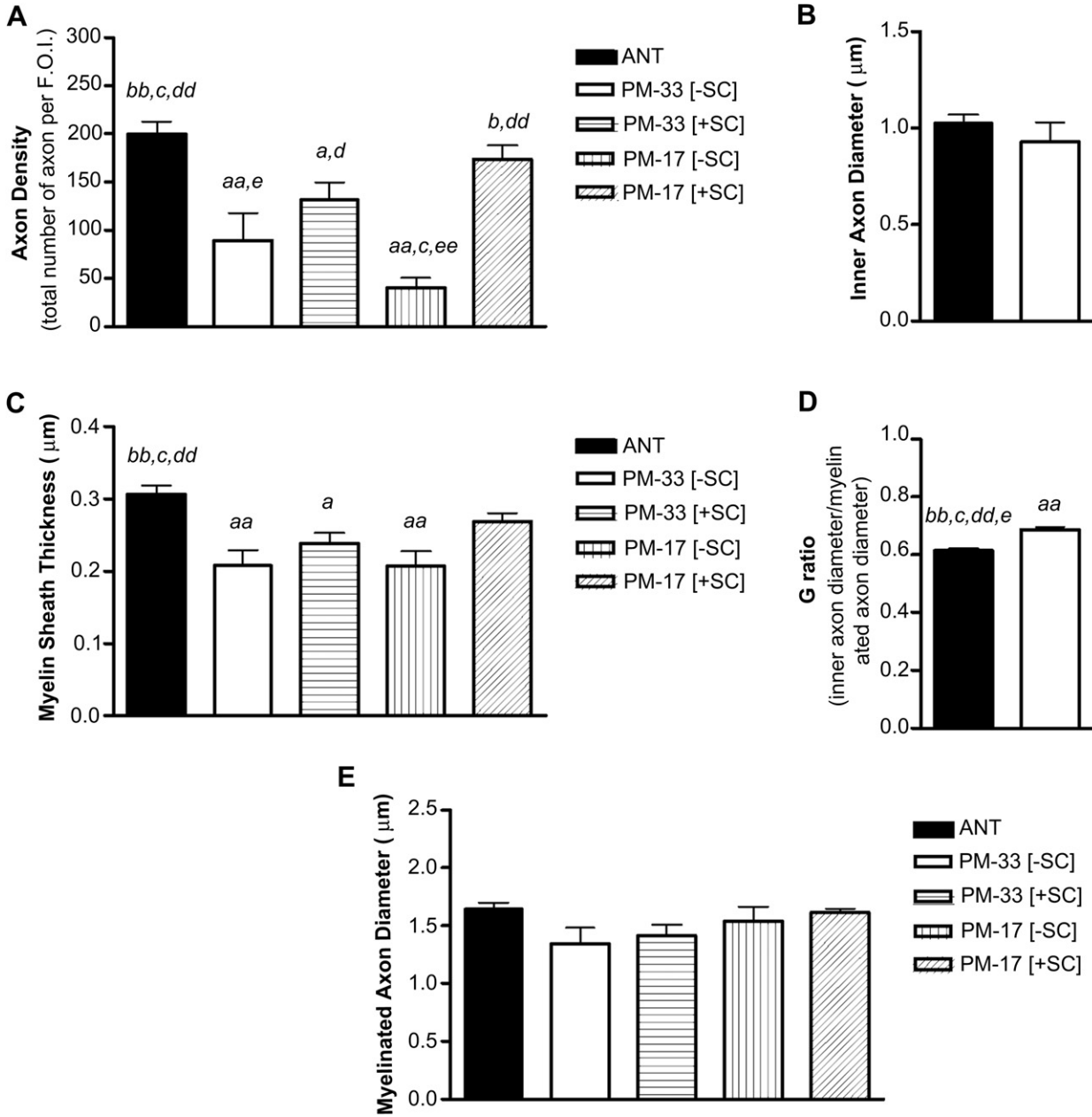

Fig. 11. Morphometric analysis of axon regeneration at 6 weeks after implantation. At the distal end of the graft, several parameters of axonal regeneration were investigated within defined fields of interest including (A) mean axon density, (B) mean inner axon diameter, (C) mean myelin sheath thickness, (D) G-ratio, and (E) mean myelinated axon diameter. Statistical analysis involved ANOVA with Tukey *post-hoc* test for multiple comparisons. [***a***: $p < 0.05$ in comparison with ANT; ***b***: $p < 0.05$ in comparison with PM-33 (−SC); ***c***: $p < 0.05$ in comparison with PM-33 (+SC); ***d***: $p < 0.05$ in comparison with PM-17 (−SC); ***e***: $p < 0.05$ in comparison with PM-17 (+SC). In case of high significance with $p < 0.01$ the letters are doubled (***aa***, ***bb***, ***cc***, ***dd***, ***ee***). ***aa***: $p < 0.05$ in comparison with ANT; ***bb***: $p < 0.05$ in comparison with PM-33 (−SC); ***cc***: $p < 0.05$ in comparison with PM-33 (+SC); ***dd***: $p < 0.05$ in comparison with PM-17 (−SC); ***ee***: $p < 0.05$ in comparison with PM-17 (+SC)].

fibres and their nodes of Ranvier (see Fig. 8). Both our Perimaix model and the multi-channel concept by Yao et al. [44] mimic characteristics of a natural nerve, but differ in pore size diameter. Theoretically, the nerve guides should have pores that are small enough to physically align and restrict the direction of growing axons. Simultaneously, the pores should be large enough to allow for vascularization and infiltration of cells that support regeneration. A key factor for 3D nerve guides is to maximize directional topographic cues while minimizing cross-sectional area occupied by material [23]. We had two reasons for choosing a mean pore size diameter of 50 μm. First, physical features are characterized by the enkapsis of the peripheral nerve (i.e. Schwann tube/endoneurium/perineurium/epineurium). The basal lamina, together with the endoneurial reticular and collagen fibres, provide the framework for supporting the nerve fibres. They are termed "Schwann tube", which are longitudinal and continuous [46]. The diameters of these Schwann tubes are mainly defined by axon diameter, which ranged from 2 to 5 μm (Aδ) to 15–20 mm (Aα). Second, our chosen pore size was chosen in agreement with a number of previous studies:

Lietz and colleagues [47] presented a nerve guide on the basis of a poly-trimethylenecarbonate-e-caprolactone (TMC-CL) tube with an inner framework consisting of poly-glycolide (PGA) filaments. They reported that longitudinally orientated micro-grooves were essential for the orientation of SC processes and axonal growth from embryonic chicken DRG. Non-orientated samples resulted only in random SC alignment and a meandering pattern of axonal growth [47]. Lane widths larger than 50μm or 100 μm were reported to induce less control of SC orientation [47]. Likewise, a recent study, in which micro-patterned groove widths of approximately 30–50 μm were reported to exert significant influence over the orientation of neurite growth. Channel widths ranging from 30 to 1000 μm, were tested [48]. In a recent publication Hu and colleagues [25] presented a multi-channeled nerve guide with a mean pore channel diameter of 37.41 ± 11.0 μm.

Another aspect of nerve guide optimization for the transfer of Perimaix technology for a possible clinical applicationinvolves the use of an epineurial replacement. In the present study, the host outer epineurium was used as a "sleeve" to hold and stabilize the Perimaix nerve guide in its position between the proximal and distal nerve stumps. Although the negative control group (i.e. fibrin cylinder [−SC]) did not reveal appropriate axonal growth, it can be discussed that the implanted Perimaix nerve guides were able to recruit endothelial cells from blood vessels in the surrounding epineurium. In fact, in a clinical setting, nerve injuries are likely to demonstrate destruction of the epineurium. Therefore, future Perimaix implantation strategies will have to develop and incorporate a component which replaces the lost epineurium. Designing an appropriate or ideal epineurial replacement requires stability without collapse or kinking, as well as optimal diffusion of nutrients and provision of tensile strength to support fixation by microsurgical sutures [22].

5. Conclusion

The axon growth supportive performance of two (collagen-based) Perimaix nerve guides has been evaluated in a 2 cm defect of the rat sciatic nerve. Seeding of the Perimaix nerve guides with SC was found to generate columns of SC which resembled Bands of Büngner and which were maintained for at least 1 week after implantation. The PM-17 + SC scaffold was found to support axon regeneration that was almost as effective as that supported by the gold standard (ANT) over a period of 6 weeks. Finally, it should be noted that the quantitative results of regeneration in our study were still best for autograft repair. It t is important to realize that the ideal alternative for the autograft should perform better than the autograft.

Acknowledgements

A. Bozkurt was supported by grants #0312758, #0313640, #0315140 from the German Federal Ministry of Education and Research (BMBF), the Science Award of the Sibylle Assmus-Foundation (Förderpreis Neuroregeneration 2009, Stiftung Sibylle Assmus) and "START" program funds provided by the Faculty of Medicine of the RWTH Aachen University of Technology. R. Deumens was funded by a grant from the Dutch Polymer Institute (DPI#608) and G. Brook was funded by the German Research Foundation (DFG, BR 2299/4-1). The authors are grateful to Mrs. Christine Beckmann for the histological preparations and morphometric measurements. The authors also thank Mrs. Astrid Knischewski and Mrs. Hannelore Mader for their technical help.

Appendix. Supplementary material

Supplementary data associated with this article can be found, in the online version, at doi:10.1016/j.biomaterials.2011.10.069

References

[1] Stoll G, Griffin JW, Li CY, Trapp BD. Wallerian degeneration in the peripheral nervous system: participation of both Schwann cells and macrophages in myelin degradation. J Neurocytol 1989;18:671–83.
[2] Chen ZL, Yu WM, Strickland S. Peripheral regeneration. Annu Rev Neurosci 2007;30:209–33.
[3] Deumens R, Bozkurt A, Meek MF, Marcus MA, Joosten EA, Weis J, et al. Repairing injured peripheral nerves: bridging the gap. Prog Neurobiol 2010; 92:245–76.
[4] Berger JV, Knaepen L, Janssen SP, Jaken RJ, Marcus MA, Joosten EA, et al. Cellular and molecular insights into neuropathy-induced pain hypersensitivity for mechanism-based treatment approaches. Brain Res Rev 2011; 67(1–2):282–310.
[5] Lee SK, Wolfe SW. Peripheral nerve injury and repair. J Am Acad Orthop Surg 2000;8:243–52.
[6] Lundborg G. Alternatives to autologous nerve grafts. Handchir Mikrochir Plast Chir 2004;36:1–7.
[7] Bellamkonda RV. Peripheral nerve regeneration: an opinion on channels, scaffolds and anisotropy. Biomaterials 2006;27:3515–8.
[8] Teng YD, Lavik EB, Qu X, Park KI, Ourednik J, Zurakowski D, et al. Functional recovery following traumatic spinal cord injury mediated by a unique polymer scaffold seeded with neural stem cells. Proc Natl Acad Sci U S A 2002;99: 3024–9.
[9] Bozkurt A, Deumens R, Beckmann C, Olde Damink L, Schugner F, Heschel I, et al. In vitro cell alignment obtained with a Schwann cell enriched microstructured nerve guide with longitudinal guidance channels. Biomaterials 2009;30:169–79.
[10] Bozkurt A, Brook GA, Moellers S, Lassner F, Sellhaus B, Weis J, et al. In vitro assessment of axonal growth using dorsal root ganglia explants in a novel three-dimensional collagen matrix. Tissue Eng 2007;13:2971–9.
[11] Mollers S, Heschel I, Damink LH, Schugner F, Deumens R, Muller B, et al. Cytocompatibility of a novel, longitudinally microstructured collagen scaffold intended for nerve tissue repair. Tissue Eng Part A 2009;15: 461–72.
[12] Inoue H, Ohsawa I, Murakami T, Kimura A, Hakamata Y, Sato Y, et al. Development of new inbred transgenic strains of rats with LacZ or GFP. Biochem Biophys Res Commun 2005;329:288–95.
[13] Vroemen M, Weidner N. Purification of Schwann cells by selection of p75 low affinity nerve growth factor receptor expressing cells from adult peripheral nerve. J Neurosci Methods 2003;124:135–43.
[14] Schoof H, Bruns L, Fischer A, Heschel I, Rau G. Dendritic ice morphology in unidirectionally solidified collagen suspensions. J Crystal Growth 2000;209: 122–9.
[15] Schmitte R, Tipold A, Stein VM, Schenk H, Flieshardt C, Grothe C, et al. Genetically modified canine Schwann cells–In vitro and in vivo evaluation of their suitability for peripheral nerve tissue engineering. J Neurosci Methods 2010;186:202–8.
[16] Bozkurt A, Deumens R, Scheffel J, O'Dey DM, Weis J, Joosten EA, et al. CatWalk gait analysis in assessment of functional recovery after sciatic nerve injury. J Neurosci Methods 2008;173:91–8.
[17] Junqueira LC, Montes GS, Krisztan RM. The collagen of the vertebrate peripheral nervous system. Cell Tissue Res 1979;202:453–60.

[18] Kaemmer D, Bozkurt A, Otto J, Junge K, Klink C, Weis J, et al. Evaluation of tissue components in the peripheral nervous system using Sirius red staining and immunohistochemistry: a comparative study (human, pig, rat). J Neurosci Methods 2010;190:112–6.
[19] Bozkurt A, Scheffel J, Brook GA, Joosten EA, Suschek CV, O'Dey DM, et al. Aspects of static and dynamic motor function in peripheral nerve regeneration: SSI and CatWalk gait analysis. Behav Brain Res 2011;219(1): 55–62.
[20] Weis J, Schroder JM. Differential effects of nerve, muscle, and fat tissue on regenerating nerve fibres in vivo. Muscle Nerve 1989;12:723–34.
[21] Schroder JM, Hoheneck M, Weis J, Deist H. Ethylene oxide polyneuropathy: clinical follow-up study with morphometric and electron microscopic findings in a sural nerve biopsy. J Neurol 1985;232:83–90.
[22] Gu X, Ding F, Yang Y, Liu J. Construction of tissue engineered nerve grafts and their application in peripheral nerve regeneration. Prog Neurobiol 2010;93: 204–30.
[23] Kim YT, Haftel VK, Kumar S, Bellamkonda RV. The role of aligned polymer fiber-based constructs in the bridging of long peripheral nerve gaps. Biomaterials 2008;29:3117–27.
[24] Clements IP, Kim YT, English AW, Lu X, Chung A, Bellamkonda RV. Thin-film enhanced nerve guidance channels for peripheral nerve repair. Biomaterials 2009;30:3834–46.
[25] Hu X, Huang J, Ye Z, Xia L, Li M, Lv B, et al. A novel scaffold with longitudinally oriented microchannels promotes peripheral nerve regeneration. Tissue Eng Part A 2009;15:3297–308.
[26] Huang J, Lu L, Hu X, Ye Z, Peng Y, Yan X, et al. Electrical stimulation accelerates motor functional recovery in the rat model of 15-mm sciatic nerve gap bridged by scaffolds with longitudinally oriented microchannels. Neurorehabil Neural Repair 2010;24:736–45.
[27] Cao J, Sun C, Zhao H, Xiao Z, Chen B, Gao J, et al. The use of laminin modified linear ordered collagen scaffolds loaded with laminin-binding ciliary neurotrophic factor for sciatic nerve regeneration in rats. Biomaterials 2011;32(16): 3939–48.
[28] Schmidt CE, Leach JB. Neural tissue engineering: strategies for repair and regeneration. Annu Rev Biomed Eng 2003;5:293–347.
[29] Pfister LA, Papaloizos M, Merkle HP, Gander B. Nerve conduits and growth factor delivery in peripheral nerve repair. J Peripher Nerv Syst 2007;12: 65–82.
[30] Bunge RP. Some observations on the role of Schwann cells in peripheral nerve regeneration. In: McCarroll Jewet, editor. Nerve repair and regeneration - its clinical and experimental basis. St Louis: Mosby; 1980. p. 58–64.
[31] Fawcett JW, Keynes RJ. Peripheral nerve regeneration. Annu Rev Neurosci 1990;13:43–60.
[32] Iwashita Y, Crang AJ, Blakemore WF. Redistribution of bisbenzimide Hoechst 33342 from transplanted cells to host cells. Neuroreport 2000;11: 1013–6.
[33] Hofstetter CP, Holmstrom NA, Lilja JA, Schweinhardt P, Hao J, Spenger C, et al. Allodynia limits the usefulness of intraspinal neural stem cell grafts; directed differentiation improves outcome. Nat Neurosci 2005;8:346–53.
[34] Deumens R, Koopmans GC, Honig WM, Hamers FP, Maquet V, Jerome R, et al. Olfactory ensheathing cells, olfactory nerve fibroblasts and biomatrices to promote long-distance axon regrowth and functional recovery in the dorsally hemisected adult rat spinal cord. Exp Neurol 2006;200:89–103.
[35] Pettersson J, Lobov S, Novikova LN. Labeling of olfactory ensheathing glial cells with fluorescent tracers for neurotransplantation. Brain Res Bull 2010;81: 125–32.
[36] Yannas IV, Hill BJ. Selection of biomaterials for peripheral nerve regeneration using data from the nerve chamber model. Biomaterials 2004;25: 1593–600.
[37] Biazar E, Khorasani MT, Montazeri N, Pourshamsian K, Daliri M, Rezaei M, et al. Types of neural guides and using nanotechnology for peripheral nerve reconstruction. Int J Nanomedicine 2010;5:839–52.
[38] Chalfoun CT, Wirth GA, Evans GR. Tissue engineered nerve constructs: where do we stand? J Cell Mol Med 2006;10:309–17.
[39] Vleggeert-Lankamp CL. The role of evaluation methods in the assessment of peripheral nerve regeneration through synthetic conduits: a systematic review. Laboratory investigation. J Neurosurg 2007;107:1168–89.
[40] Liu BS, Yao CH, Hsu SH, Yeh TS, Chen YS, Kao ST. A novel use of genipin-fixed gelatin as extracellular matrix for peripheral nerve regeneration. J Biomater Appl 2004;19:21–34.
[41] Lee AC, Yu VM, Lowe 3rd JB, Brenner MJ, Hunter DA, Mackinnon SE, et al. Controlled release of nerve growth factor enhances sciatic nerve regeneration. Exp Neurol 2003;184:295–303.
[42] Keilhoff G, Stang F, Wolf G, Fansa H. Bio-compatibility of type I/III collagen matrix for peripheral nerve reconstruction. Biomaterials 2003;24:2779–87.
[43] Stang F, Fansa H, Wolf G, Reppin M, Keilhoff G. Structural parameters of collagen nerve grafts influence peripheral nerve regeneration. Biomaterials 2005;26:3083–91.
[44] Yao L, de Ruiter GC, Wang H, Knight AM, Spinner RJ, Yaszemski MJ, et al. Controlling dispersion of axonal regeneration using a multichannel collagen nerve conduit. Biomaterials 2010;31:5789–97.
[45] Brushart TM, Mathur V, Sood R, Koschorke GM, Joseph H. Boyes Award. Dispersion of regenerating axons across enclosed neural gaps. J Hand Surg Am 1995;20:557–64.
[46] Millesi H, Terzis JK. Nomenclature in peripheral nerve surgery. Committee report of the international society of reconstructive microsurgery. Clin Plast Surg 1984;11:3–8.
[47] Lietz M, Dreesmann L, Hoss M, Oberhoffner S, Schlosshauer B. Neuro tissue engineering of glial nerve guides and the impact of different cell types. Biomaterials 2006;27:1425–36.
[48] Goldner JS, Bruder JM, Li G, Gazzola D, Hoffman-Kim D. Neurite bridging across micropatterned grooves. Biomaterials 2006;27:460–72.